



# Experimental investigations on silicon carbide mixed electric discharge machining

Surendra Singh Thakur<sup>1</sup> · Sharad K. Pradhan<sup>2</sup> · Shankar Sehgal<sup>3</sup> · Kuldeep K. Saxena<sup>4</sup>

Received: 21 March 2022 / Accepted: 19 June 2022 / Published online: 30 July 2022  
© Springer Nature B.V. 2022

## Abstract

In this study, silicon carbide mixed electrical discharge machining (SCMEDM) process has been developed and later on modelled also using an artificial neural network (ANN) based technique as well as response surface methodology (RSM). Experiments were conducted with Al LM-25/SiC metal matrix composites as per Box Behnken design (BBD). Discharge current, pulse-on-time, servo-voltage, powder concentration, tool material and varying reinforcement levels were considered as machining input parameters. Material removal rate, tool wear rate and surface roughness were taken to be the response parameters. Analysis of variance (ANOVA) method was used to investigate the significant effect of parameters on the response measures. The experimental data was trained using a back-propagation ANN technique. Research shows that the influence of current, pulse length and tool material on the machining characteristics of Al LM-25 MMCs is significant. Surrogated models were also developed for proposed process using RSM. However, the accuracy of ANN models was found to be better than that of RSM models.

**Keywords** Silicon carbide mixed electrical discharge machining (SCMEDM) · Artificial neural network (ANN) · Analysis of variance (ANOVA) · Response surface model (RSM)

## Abbreviations

ANN	Artificial neural network
RBFNN	Radial Basics Function Neural Network
NSGA	Non sorting genetic algorithm
SCMEDM	Silicon carbide mixed electro discharge machining
WEDM	Wire electro discharge machining
FEM	Finite element method
DEM	Dimensional exponential model
TWR	Tool wear rate

SF	Surface finish
CR	Crater radius
$\rho_w$	Density of work piece material
$K_w$	Work piece thermal conductivity
Vg	Voltage Gap
$T_{ON}$	Pulse-on-time
$T_{OFF}$	Pulse-off-time
Ra	Surface Roughness
$R^2$	Coefficient of determination
BPNN	Back propagation neural network
ANOVA	Analysis of variance
PCA	Principal Component Analysis
MMC	Metal matrix composites
SEM	Scanning electron microscopy
MRR	Metal removal rate
SR	Surface roughness
OC	Over cut
SEM	Scanning electron microscope
$I_p$	Input Current
$\alpha_w$	Thermal expansion coefficient
Cp	Concentration of powder
WT	White layer thickness
PMEDM	Powder mixed electro discharge machining

✉ Surendra Singh Thakur  
thakur\_surendra2003@rediffmail.com

<sup>1</sup> Sr. Project Engineer, Siemens and 3D Engineering Pvt. Ltd, Pune, MH, India

<sup>2</sup> Department of Mechanical Engineering, National Institute of Technical Teachers' Training and Research Bhopal, Madhya Pradesh, India

<sup>3</sup> Mechanical Engineering, UIET, Panjab University, Chandigarh, India

<sup>4</sup> Department of Mechanical Engineering, GLA University, Mathura, UP 281406, India

## 1 Introduction

Metal matrix composites (MMC) have rapidly penetrated into numerous industries including aerospace, defence, manufacturing, automobile, electronic and nuclear [1]. Due to their favourable properties such as light in weight, better wear resistance, better specific strength and temperature resistance than conventional materials [2], they are extensively used in many industrial applications. In the realm of industrial production, conventional machining approaches generally are insufficient to machine MMC for achieving the required precision and intricate shapes, which are also time-consuming and sometimes difficult to machine [3–5]. An advanced manufacturing process is the only way to achieve such features on a component. In the recent past, Electrical discharge machining (EDM) has been gaining attention as a significant technology for cutting several hard and difficult-to-machine materials due to the intense heating made by controlled, localized electric sparks and produces negligible stress (minimum surface tension) on the workpiece surface to remove material. Thus, by considering the most appropriate and optimal process parameters, which mostly consume precious time and effort, the EDM process becomes more effective in terms of cost, quality and productivity than traditional machining of difficult-to-cut materials. As a result of the effective utilization of experimental, modelling and optimization methodology, a new technological solution is able to meet and control multiple objectives simultaneously (multi-objective) in order to provide optimized machining of advanced MMCs. Many statistical and computational approaches have been used for predictive modelling, including RSM [6–11], ANN [12–17], Taguchi method [18–21], GRA [22–26], desirability function approach of RSM [27–30], PCA [31, 32], TOPSIS [33–35], GA [36–39] and PSO [40–43]. The machinability of various materials has been extensively explored by employing various experimental design, numerical modelling approaches and optimization techniques [44–47]. The objective was to estimate the performance and to modify the input factors in cutting the materials like Stainless steel, A2 tool steel, Grey cast iron, Inconel 600, 601, 625, 825, 718, MDN 300, AISI D2, D3, D6, AISI 316 L, Ti6Al4V, Ti13Zr13Nb, nickel alloy, Al7075, Al6061, Al6063 alloy, Al-SiC MMC, Si<sub>3</sub>.

## 2 Literature Review

Several publications applying one out of statistical or computational technique rather than considering both to solve multi-objective problems, which are crucial in improving

machining performance. Hence, appropriate technological guideline is required to be developed for effective and optimum machining of LM-25/SiC MMC material by SCMEDM process. Because of its extreme strength at high temperatures, excellent corrosion resistance and exceptional wear resistance.

However, until now, no author has performed any economic analysis facilitating cost-effective manufacturing based on SCMEDM that can provide scope for further researches related to techno-economic aspect. The current investigation handles sustainability assessment of EDM processes so as to analyze the machining efficiency of silicon carbide mixed electrical discharge machining of LM-25/SiC MMC with respect to MRRs, TWRs and SRs by employing process parameters (discharge current, gap voltage, pulse-on-time, powder content, tool material and reinforcement percentage). Experimental investigations, prediction models and optimal design of multi-responses are investigated using Box-Behnken's (BBD) design, ANOVA and statistical techniques. Afterward, an artificial neural network (ANN) is employed as a computational model for multi-response optimization. In addition, a best-fit economic analysis is used to determine the suitability of PMEDM for difficult-to-cut materials [2, 48] as well as hard-to-cut materials [49, 50], with the purpose of raising manufacturing industry awareness. SEM observation helped interpret the results by investigating the impact of discharge current on machined surface morphology, recast layer thickness and crack width on the SCMEDM work surface thickness and crack length. This study provides a method for assessing sustainability while considering the machining performance from the perspective of novelty; these results can help establish an economic advantage for SCMEDM in industries such as automotive, aerospace, military and electrical. Mentioned points make the present study unique and will lead to a significant contribution to advance sustainable manufacturing (Table 1).

Reviewing the literature reveals that ANN is frequently used in modelling and process optimization. It is able to build nonlinear relationships between a large variety of input and output parameters. An ANN can be trained on any number of data sets and it is capable of maintaining implicit relationships between inputs and outputs implicitly, unlike mathematical models which are data-driven, self-adaptive and rigid. Furthermore, artificial neural networks can be trained on a wide range of data sets and they can infer complex nonlinear functional relationships between inputs and outputs implicitly. Most research uses a single-hidden-layer ANN architecture, thus, the accuracy of the resulting model has received less attention. Further, the previous work did not consider composites, notably LM-25/SiC composites, as a work item. Despite the fact that tool material is a key parameter, it can affect the accuracy of SCMEDM [70].

**Table 1** Research contribution on ANN modelling

Author(s)	Prediction approach	Work Piece	Process variable	Machine response	Result
Shrivastava et al. [51]	ANN and RSM	copper-iron graphite MMC	Ton, T <sub>off</sub> , Ip, Grit no	MRR,SR	RSM and ANN are both more reliable and competent methods for estimating the average SR
Rajesh et al. [52]	RSM, Radial Basics Function Neural Network (RBFNN) and ANN	LM-25 Al composites	V <sub>d</sub> , Ip, Ton, T <sub>off</sub> , Sg, P <sub>oil</sub>	MRR,SR	Prediction model RSM,RBFNN and ANN predict the error by RSM is 1.34655%,RBFNN is 1.5236% and the ANN model is 0.7878%
Surya et al. [53]	RSM and ANN	Wire EDM of Al7075-TiB <sub>2</sub> in-situ composites	Ton, T <sub>off</sub> , Ip, S	MRR, CR, DE	70% of the training set correlated well with the observed values, according to an ANN
Dubey et al. [54]	RSM	Al7075-5% B <sub>4</sub> Cp metal matrix composites	V <sub>g</sub> , Ton, T <sub>off</sub> , Ip,	TWR, SR	In Additive mixed electrical discharge machining Pulse off-time had a negligible effect on Ra
Phate et al. [55]	RSM,integrated PCA-ANN	Aluminium silicate composites with a silicate content of 15–20% (Al/SiCp)	P <sub>ON</sub> , P <sub>OFF</sub> , Ip, WFR,WT,FP,SIC (%)	MRR, Ra, KRF	Essential process parameters are the silicate percent composition, the pulse off time (POFF) and the current (IP)
Preetham et al. [56]	RSM	Aluminium metal matrix hybrid composites	Ton, T <sub>off</sub> , Wt, F,	Ra	Pulse length (pulse on time) had the biggest influence on the work piece's surface integrity
S. Singh et al.[57]	RSM and ANN	LM-25/SiC MMC	Ton, T <sub>off</sub> , Ip,	MRR,TW,SR	SCMEDM is mostly influenced by current intensity and pulse duration
Singh et al. [58]	Back-propagation algorithm and RSM	D3 die steel using ANNs	Ton, Ip, duty cycle, Pg and electrode rotation	MRR, SR	Presented mathematical models for predicting MRR and SR during helium-assisted EDM machining of with a
Agrawal et al. [59]	ANN and GA	Copper-iron-carbide MMC	Ton, T <sub>off</sub> , Ip, powder con. (g/l)	MRR, Ra	Ton significantly affect the MRR
Kumar and Chouhan [60]	RSM and ANN	Al7075/10/SiCp and Al 7075 hybrid composites	Cutting speed, feed rate, approach angle	Ra	Cutting speed has significant factor for Ra
Bhuyan et al. [61]	fuzzy logic and RSM	Al-SiCp MMC	T <sub>ON</sub> , I <sub>p</sub> and F <sub>p</sub>	R <sub>a</sub> ,R <sub>q</sub> and R <sub>z</sub>	Ip has more impact of Ra
Kumar & Sreebalaj[62]	ANN	Al MMC with fly ash particles	T <sub>ON</sub> , T <sub>OFF</sub> and Ip	MRR, TWR and SR	T <sub>ON</sub> , T <sub>OFF</sub> has significantly effect on MRR
Unune et al. [63]	Fuzzy logic	Nimonic 80A	I <sub>p</sub> , T <sub>OFF</sub>	MRR, R <sub>a</sub>	MRR increases with increase in both I <sub>p</sub> & T <sub>OFF</sub>
Sahu et al. [64]	RSM and ANN	Al-SiC MMC	I <sub>p</sub> , V, T <sub>ON</sub> , T <sub>OFF</sub> and flushing pressure	R <sub>a</sub> and OC	V, T <sub>OFF</sub> and flushing pressure are significant parameters in affecting Ra
Ubale et al. [65]	BPNN with one -hidden layer	70 wt% W- 30 wt% Cu MMC	I <sub>p</sub> , T <sub>ON</sub> , T <sub>OFF</sub> , Wt and Gp	MRR	5–12-1 best model selected for modelling the MRR

Table 1 (continued)

Author(s)	Prediction approach	Work Piece	Process variable	Machine response	Result
Lalwani et al. [66]	RSM, ANN and NSGA- II	Inconel 718 super alloy	$T_{ON}$ , $T_{OFF}$ , SV, $I_p$ and WT	Kf, $R_a$ and MRR	ANN model predict better MSE value for ANN (1.49%) and RSM (5.71%)
Mamikandan et al. [67]	ANFIS	LM6/SiC/ Dumite HMMC	$T_{ON}$ , $T_{OFF}$ , Wf, SV, and flushing pressure	MRR), Ra, overcut, circularity error	$T_{ON}$ has most influencing parameter for machining of WEDM of LM6/ SiC/Dumite HMMC
Singh et al. [68]	RSM	hybrid aluminium MMC with SiC/ Gr	I, V, $T_{on}$ and tool material,	MRR, Ra	MRR and the Ra significantly influenced by both Copper and Brass electrodes
Phate et al. [69]	DEM, RSM and ANFIS	aluminium-based alloy	$T_{ON}$ , $T_{OFF}$ and $I_p$	Roughness (Ra)	' $I_p$ ' is most affecting parameter followed by the ' $T_{ON}$ ', ' $T_{OFF}$ ' and ' $CP$ '

Earlier research did not take account of it while modelling this process.

### 3 Experimentation

#### 3.1 Silicon Carbide Mixed Electrical Discharge Machining (SCMEDM)

Researchers have demonstrated that SCMEDM increases the speed of EDM based machining SCMEDM is an advanced machining technique that mixes a fine, abrasive, electrically conductive powder with the dielectric medium. Metallic powders suspended in a dielectric medium reduce the insulating strength of the material, resulting in a higher inter electrode gap. These results in improved EDM performance like higher MRR reduce TWR and SR than regular EDM. Figure 1 depicts the schematic of SCMEDM.

In PMEDM suitable powder SiC is chosen to mix with the dielectric liquid in a controlled set-up with pumping device. The powder is mixed using a stirrer for complete mixing in the dielectric liquid and pump ensures that it so not get settled in the tank. Similar to conventional EDM thermal energy is generated at the junction of electrode and job with the help of high voltage electrical sparks. Due to presence of powder the electrical density at the machining spot decreases which in turn forces the thermal energy produced to raise the local temperature to a higher value thereby melting and vaporising the job material. To avoid excessive heating short pulses are used. PMEDM involves adding conductive powders to achieve an increased MRR, SF and tool life by causing dielectric liquid to breakdown earlier [71]. Conduit powders such as copper [71], aluminium [70–72] of various sizes, chromium [73], silicon carbide [74], CNT [75], manganese [76], boron carbide [77], graphene nano powder [78], graphite [79] and others, when added to the dielectric liquid will results in higher MRR and reduced SR. By mixing powder with dielectric liquid, the MRR can be increased by 1% to 33% without compromising quality [80]. In one study [81], an increase in MRR due to non-uniform heat dissipation was identified, resulting in the dissipation of surplus residual heat.

Al powders in the appropriate proportion are mixed with dielectric liquid to enhance the responses [82]. As per during machining of aluminium composite with copper electrodes, addition of aluminium powder in specified quantities to dielectric liquid leads to better MRR and SR [72]. The appropriate addition of CNTs to EDM's dielectric liquid increases its machining rate and reduces the SR [83]. Nano-almond powder significantly improved titanium alloy surface quality for biomedical applications by forming carbon-enriched surfaces for better osseointegration [70]. A CNT additive was found to reduce micro crack formation and improve the

**Fig. 1** ZNC EDM machine ELECTRA PLUS, (Model S-50 ZNC)



stability of machining [75]. Adding chromium to dielectric liquid produces a chromium-rich machined surface [84]. To improve the SR, the powder concentration needs to be controlled [77]. Depending on the workpiece and surface finish of the components, proper identification of powder size and concentration can yield a mirror finish [85]. Chromites powders in an appropriate size and concentration reduce SR and cracks and reduce crater size when machining H-11 die steel [73]. The micro hardness of the machined surface must also increase with an increase in powder concentration. A proper choice of powder concentration can yield better results [86]. Micro hardness is measured when manganese powder is mixed with dielectric liquid during machining of OHNS die steel. A maximum of 8% of the powder can be added in proportion to dielectric liquid [70]. Multi walls of CNT increased MRR until 8 gm/lit of powder concentration was reached [80]. When machining H11 die steel, the ability of materials to transfer current effectively increased MRR. SR reduced until SiC powder concentration of 4 gm/lit was achieved. Due to addition of SiC in the dielectric liquid, the transfer of material from electrode to job was of small quantity [87]. Dubey et al. [54] experimented on Al7075–5%B<sub>4</sub>Cp metal matrix composite by incorporating chromium powder in machining. Higher peak current and pulse on time increase the height of recast layers. Singh et al. [88] implemented RSM & ANN technique to estimate experimental inputs and modelling of measure response such as MRR, TW, and SR. It is observed that predicted results from ANN model are compared with experimental result are quite satisfactory. Naiket al. [89] Response surface methodology (RSM) and analysis of variance (ANOVA) are employed,

respectively, for experimental analysis, predictive modelling in electrical discharge machining process for aluminium–silicon carbide metal matrix composite. Result reveal that discharge current have major influence on machined surface. Phate et al. [90] have employed the Artificial Neural Network (ANN)-Based PCA technique for analysing processes and enhancing the process performance. From the investigation. It is observed that the % composition of silicate, the pulse off time (POFF) and current (IP), are the most critical process parameters. Ming et al. [91] proposed a multi-variable regression model using back propagation neural network (BPNN) and a radial basis neural network (RBNN) to model and optimize die sinking EDM process of SiC/Al composites. Padhee et al. [92] A response surface methodology (RSM) has been used to analyze the effects of independent variables on the results and develop Non-sorted genetic algorithms (NSGA) for investigating the machining performance of power mix EDM using EN 31 steel. Tall et al. [93] observed MRR of the Al/Al<sub>2</sub>O<sub>3</sub> composite with EDM can be improved by adding aluminium powder in the dielectric liquid. Kolli et al. [94] found that adding graphite powder (14 g/L) and surfactant (varying between 0.25 and 15.0 g/L) to a dielectric fluid when EDMing titanium alloy improved the MRR. Kansal et al. [95] observed that the machining rate of die steel has been improved by adding silicon powder (average particle size 30 nm) in the dielectric fluid, in particular an increase from 2.67 to 4.58 mm<sup>3</sup>/min was reported at a 3 g/L concentration of Si powder. According to Singh et al. [96], the highest MRR was found when silicon powder was diluted by 8 g/L PMEDM. In Kumar et al. [97] studied that during PMEDM

of the Al-SiCP MMC, peak current, powder concentration and pulse duration are the influencing factors. The authors observed that reinforcement of 10% SiC particles (average size of 25  $\mu\text{m}$ ) with 4 g/L silicon powder concentration results in a higher MRR of 2.93  $\text{mm}^3/\text{min}$ . According to the PMEDM studies [98–103] a higher powder concentration in dielectric liquids improves machining performances. Tripathy et al. deployed TOPSIS and GRA techniques to assess the efficacy of chromium powder mixed EDM with copper electrode for machining H-11 die steel. Experimental results indicate that adding a proper concentration of particles of the proper size improves SF [104]. Kansal et al. [105] have demonstrated that a novel nano porous layer generated by PMEDM techniques can enhance the biomechanical anchorage of bone-implant structures. Tripathy and Tripathy [106] studied chromium powder mixed EDM to investigate the effect of process variables on micro hardness in H-11 die steel and estimate the migrated material from workpiece to tool depending on peak current, powder concentration, duty cycle and pulse time employing SEM and EDS. Nanimina et al. [107]. Experimental results showed that using nano aluminium powder as a matrix in EDM to machine Ti6Al4V workpieces with a copper-tungsten electrode improved SF by reducing micro cracks and craters. Surface restoration is improved due to uniform distribution of silver particles and a carbide-rich surface layer formed by alloying of transfer elements. Hamidullah et al. [108] studied the effect of SiC powder concentration on particle deposition, subsurface structures and surface topography during PMEDM of Ti-6Al-4 V-ELI material and concluded that the material transfer mechanism improves with low pulse currents and higher suspended particle concentration. Kumar et al. [109] investigated machining of Inconel 825 workpieces using  $\text{Al}_2\text{O}_3$  micro PMEDM machining. It was determined that discharge current, pulse duration and voltage are the major parameters affecting MRR and SR. Rajavel et al. [110] presented a comprehensive review of EDM of various composite materials. Saharia et al. [111] studied Hybrid PMEDM with Multi-Walled Carbon Nano Tube (CNT) powders and kerosene for grinding EN19 alloy steel parts with brass electrodes. Surekha, et al. [112] investigated experimentally the use of aluminium powder in EDM with brass electrodes for machining EN-19 alloy steel and concluded that gap voltage and peak current affect MRR significantly.

### 3.2 Material of the Work Piece

An abrasive tool was used to machine LM-25/SiC reinforced composite material and developed work piece specimens with dimensions of 150 × 15 × 10 mm (Length × Width × Thickness). Semi-automatic polishing equipment is used to polish the specimens to get a consistent surface quality on each one. The chemical composition of Al LM-25(Wt %)

composite material includes: Al 92.3812, Cu 0.0944, Mn 0.2396, Ni 0.662, Si 0.243, Fe 0.032, Zn 0.005, Pb 0.002, Sn 0.070 and C6. The mechanical properties are Density 2,680  $\text{kg}/\text{m}^3$ , Ultimate tensile strength 282 MPa, Percent elongation 5, Brinell hardness number 92 BHN and Modulus of elasticity 71 GPa.

### 3.3 Experimental Details

Figure 1 illustrates the schematic perspective in its entirety. ELEKTRA PLUS Model S-50 ZNC, Pune, India PMEDM is utilised to conduct experimentation. When a sample of the required size is prepared from an LM-25 reinforced composite alloy containing 0%, 5% and 10% by weight of silicon carbide reinforced material with a size of 30 microns (280 mesh), it exhibits superior wear resistance, high specific strength, low density and high stiffness while also exhibiting excellent thermal and shock resistance. A cylindrical electrode ( $\phi 12$  mm) was employed as a negative-polarity electrode and EDM oil was used as the dielectric liquid in this experiment. During the tests, both electrodes were kept in a silicon carbide mix dielectric to keep them from corroding.

## 4 Experimental Method

### 4.1 Experimental Design with RSM

Regression analysis has been carried out using commercial statistical software (Minitab 19) to model the response variables. The impact of process parameters on performance factors are modelled and estimated using an ANOVA test [113, 114]. ANOVA is also used to investigate the significance of the developed models to estimate the significance level of input parameters; interaction and quadratic terms [115, 116]. To establish the adequacy and prediction capabilities of the developed empirical models, correlation coefficient  $R^2$ , adjusted  $R^2$  and predicted  $R^2$  were used [117].

This research work is focused to evaluate the impact of six machining parameters (discharge current, servo power, pulse-on-time, tool material, % reinforcement and powder concentration) on machine performance, including the MRR, TWR and SR during silicon carbide mix EDM machining of LM-25/SiC composites. According to Box Behnken designs [118] a total of 54 experiments are required to estimate the impact of six machining parameters on machine response. Each experiment will be replicated once. Table 2 and 3 show the input parameters and experimental results for the TWR, MRR, and Ra, which are averages of values derived in both runs. The current set of input parameters was chosen after performing literature research, evaluating mechanism competence and taking machine constraints into account. In order to establish a mathematical relationship between

**Table 2** Process variables and their levels

Process variables	Unit	Symbols	Optimum level		
			Min	Centre	Max
			-1	0	1
Discharge Current (Ip)	Ampere	A	2	3	4
Pulse on time (Ton)	Micro second	B	30	50	75
Servo Voltage (Vs)	Volt	C	50	60	70
Con. of powder	gm/ltr	D	0	2	4
Tool Material	-	E	Brass	Copper	Graphite
% Reinforcement	-	F	LM-25	LM-25–5%SiC	LM-25–10%SiC

the dependent and independent variables, response surface methodology was applied [119]. Using RSM, the number of experimental trials can be reduced to some extent and hence, their interactions can be studied effectively.

Generally, the second-order regression model shown in Eq. 1 is used in response surface methodology.

$$Y = \beta_0 + \sum \beta_i X_i + \beta_{ii} X_i^2 + \beta_{ij} X_i X_j + \epsilon \tag{1}$$

Y represents the predicted response;  $X_i$  is the input variables,  $X_{ii}^2$  and  $X_i X_j$  is the square and constant term, respectively. The unknown regression coefficients are  $\beta_0$ ,  $\beta_i$ ,  $\beta_{ii}$  and  $\beta_{ij}$  and  $\epsilon$  is the error. Experimental work has been performed to examine the impact of different EDM input parameters such as discharge current, servo voltage, pulse on time, powder concentration, different types of tool material and different weight fraction of work material on machining performance viz. MRR, TWR, SR. The parametric level is coded using the equation.

$$\text{Coded value } (z) = \frac{X - \frac{X_{max} + X_{min}}{2}}{\frac{X_{max} - X_{min}}{2}} \tag{2}$$

As shown in Eq. 2, Z represents the coded value (-1, 0, 1). The values  $X_{max}$  and  $X_{min}$  are the maximum and minimum values of actual parameters and the actual value X is the value of the parameter.

## 5 Results and Discussion

### 5.1 Analysis of Variance

The accuracy of the developed models was evaluated with an ANOVA test using Minitab 19 Software. The results are presented in Tables 4, 5, and 6 using the response surface models of MRR, TWR, and SR, described in the following sections. In this study, the adequate criterion was  $R^2$ , adjusted  $R^2$  and anticipated  $R^2$ , all of which were around one, suggesting that the models were appropriate and fit the

data well. MRR has an  $R^2$  of 86.83%, TWR has an  $R^2$  of 84.43% and Ra has an  $R^2$  of 80.34%. Through this backward elimination procedure, insignificant terms can be removed from fit quadratic models, and the lack of fit test will not appear significant. Following the backward elimination process, the final quadratic response based analysis was performed.

ANOVA Table 4 shows that the most significant influencing factor for MRR is the tool material with a contribution of 11.90%, followed by powder concentration, servo voltage, discharge current, pulse-on-time, and % reinforcement, with contributions of 7.15%, 5.02%, 4.04% and 3.24%, respectively. In addition, the coefficient of determination ( $R^2$ ) and adjusted ( $R^2$ ) values are 86.83%, and 83.38% respectively, which indicates close alignment between the coefficient of determination ( $R^2$ ) and 77.13% significance level of the model. The lack of a fit test was deemed less significant than intended for MRR.

Further, Table 5 shows that the most influential parameter for TWR is pulse on time, which contributes 6.94%. Other important considerations include powder concentration, discharge current, servo voltage, % reinforcement and tool material, which contribute 5.55%, 4.61%, 4.09%, 3.80% and 3.22%, respectively. In general, the coefficients of determination ( $R^2$ ) and adjusted ( $R^2$ ) values of 84.43% and 80.35% are in agreement with the experimental results.

According to ANOVA Table 6, tool material is the most significant parameter for SR (11.90%). It is followed by servo voltage, powder concentration, pulse on time, discharge current and % reinforcement percentage contribution (6.07%, 5.15%, 2.46%, 2.02% and 1.49%). The value of the coefficient of determination ( $R^2$ ) 80.34% is reasonable agreement with the adjusted ( $R^2$ ) 76.24% respectively. This results in the not significant lack of fit being beneficial for SR.

According to this study, the anticipated  $R^2$  and the modified  $R^2$  were both in agreement with one another. The lack of fit was not statistically significant for each of the examples. A coefficient of variation (CV) number less than 0.41 indicates that the studies are more accurate and consistent.

**Table 3** Experimental run with process parameters and machine response

Sr.No	Run no	Ip amp	Ton μs	V volt	Powder con gm/ltr	T tool	W work	MRR (mm <sup>3</sup> /min)	TWR (mm <sup>3</sup> /min)	SR (μm)
1	1	-1	-1	0	-1	0	0	1.86567	0.03348	5.104
2	2	1	-1	0	-1	0	0	2.25835	1.84642	9.723
3	3	-1	1	0	-1	0	0	2.89164	2.11116	8.535
4	4	1	1	0	-1	0	0	3.21343	3.50334	9.677
5	51	-1	-1	0	1	0	0	2.582	3.09062	9.967
6	52	1	-1	0	1	0	0	3.14328	3.59285	9.885
7	53	-1	1	0	1	0	0	3.71194	3.96696	9.456
8	54	1	1	0	1	0	0	4.24119	4.72232	10.64
9	13	0	-1	-1	0	-1	0	0.10925	1.54581	7.592
10	14	0	1	-1	0	-1	0	0.82119	2.9229	8.607
11	15	0	-1	1	0	-1	0	0.18462	2.5629	7.757
12	16	0	1	1	0	-1	0	0.61819	3.13436	8.839
13	17	0	-1	-1	0	1	0	2.46865	2.8584	6.394
14	18	0	1	-1	0	1	0	3.11925	3.6761	9.885
15	19	0	-1	1	0	1	0	3.4258	3.86991	9.044
16	20	0	1	1	0	1	0	3.8225	4.56991	9.742
17	9	0	0	-1	-1	0	-1	0.16656	2.63348	6.583
18	10	0	0	1	-1	0	-1	1.20894	2.92232	9.884
19	43	0	0	-1	1	0	-1	0.46776	3.04464	10.83
20	44	0	0	1	1	0	-1	1.42314	3.8558	9.847
21	11	0	0	-1	-1	0	1	0.1985	0.73348	6.499
22	12	0	0	1	-1	0	1	1.20297	1.51116	9.092
23	45	0	0	-1	1	0	1	1.32313	1.52232	9.432
24	46	0	0	1	1	0	1	2.55119	1.84464	8.661
25	5	-1	0	0	-1	-1	0	0.30144	1.0229	9.278
26	6	1	0	0	-1	-1	0	0.52388	2.53436	9.849
27	47	-1	0	0	1	-1	0	1.61731	1.378	7.142
28	48	1	0	0	1	-1	0	2.64328	1.9771	9.813
29	7	-1	0	0	-1	1	0	1.78656	0.63274	8.697
30	8	1	0	0	-1	1	0	2.20716	1.98973	9.831
31	49	-1	0	0	1	1	0	2.72895	1.37168	10.85
32	50	1	0	0	1	1	0	3.51462	2.88938	10.63
33	27	0	-1	0	0	-1	-1	0.03731	0.8229	10.33
34	28	0	1	0	0	-1	-1	0.07626	1.83348	10.93
35	29	0	-1	0	0	1	-1	0.05462	0.54424	8.457
36	30	0	1	0	0	1	-1	0.5231	1.80973	9.557
37	31	0	-1	0	0	-1	1	0.03231	0.0229	7.132
38	32	0	1	0	0	-1	1	0.16119	0.81145	7.782
39	33	0	-1	0	0	1	1	0.07462	0.04424	7.478
40	34	0	1	0	0	1	1	0.16925	0.74424	8.209
41	35	-1	0	1	0	0	-1	0.07731	0.01116	7.249
42	36	1	0	-1	0	0	-1	0.18119	0.22232	8.819
43	37	-1	0	1	0	0	-1	0.46831	0.07116	6.463
44	38	1	0	1	0	0	-1	1.48656	0.08116	9.192
45	39	-1	0	-1	0	0	1	0.13731	0.08232	5.394
46	40	1	0	-1	0	0	1	1.41656	0.01116	5.471
47	41	-1	0	1	0	0	1	1.96104	0.72232	7.946
48	42	1	0	1	0	0	1	2.38059	1.65089	9.996
49	21	0	0	0	0	0	0	0.22388	0.04464	8.153
50	22	0	0	0	0	0	0	0.21656	0.03348	4.788



**Table 3** (continued)

Sr.No	Run no	Ip amp	Ton μs	V volt	Powder con gm/ltr	T tool	W work	MRR (mm <sup>3</sup> /min)	TWR (mm <sup>3</sup> /min)	SR (μm)
51	23	0	0	0	0	0	0	0.2485	0.01116	4.711
52	24	0	0	0	0	0	0	0.25626	0.03348	4.432
53	25	0	0	0	0	0	0	0.02631	0.01116	8.131
54	26	0	0	0	0	0	0	0.01274	0.01116	6.073

**Table 4** Summary of ANOVA table for MRR

Source	DF	Adj SS	Adj MS	F-Value	P-Value
Model	11	75.7428	6.8857	25.17	0.000
Linear	6	36.1532	6.0255	22.03	0.000
A-Discharge Current	1	7.9162	7.9162	28.94	0.000
B-Pulse on Time	1	7.1460	7.1460	26.12	0.000
C-Servo Voltage	1	6.5938	6.5938	24.10	0.000
D-Con. of powder	1	4.9667	4.9667	18.16	0.000
E-Tool Material	1	13.0456	13.0456	47.69	0.000
F-% reinforcement	1	0.6530	0.6530	2.39	0.130
Square	5	46.5016	9.3003	34.00	0.000
A*A	1	8.9394	8.9394	32.68	0.000
B*B	1	8.7675	8.7675	32.05	0.000
C*C	1	7.2178	7.2178	26.38	0.000
D*D	1	10.0194	10.0194	36.63	0.000
F*F	1	7.6255	7.6255	27.87	0.000
Error	42	11.4897	0.2736		
Lack-of-Fit	36	11.3161	0.3143	10.87	0.003
Pure Error	6	0.1736	0.0289		
Total	53	87.2325			

**Table 5** Summary of ANOVA table for TWR

Source	DF	Adj SS	Adj MS	F-Value	P-Value
Model	11	88.928	8.0844	20.70	0.000
Linear	6	48.556	8.0926	20.72	0.000
A-Discharge Current	1	1.365	1.3652	3.50	0.068
B-Pulse on Time	1	19.566	19.5656	50.10	0.000
C-Servo Voltage	1	18.338	18.3381	46.96	0.000
D-Con. of powder	1	17.668	17.6680	45.25	0.000
E-Tool Material	1	1.320	1.3199	3.38	0.073
F-% Reinforcement	1	3.676	3.6762	9.41	0.004
Square	5	62.776	12.5552	32.15	0.000
A*A	1	0.881	0.8812	2.26	0.141
B*B	1	23.632	23.6321	60.52	0.000
C*C	1	19.125	19.1249	48.98	0.000
D*D	1	27.271	27.2713	69.84	0.000
F*F	1	7.668	7.6681	19.64	0.000
Error	42	16.401	0.3905		
Lack-of-Fit	36	15.599	0.4333	3.24	0.072
Pure Error	6	0.802	0.1336		
Total	53	105.329			

**Table 6** Summary of ANOVA table for SR

Source	DF	Adj SS	Adj MS	F-Value	P-Value
Model	13	112.778	8.6752	7.09	0.000
Linear	6	47.247	7.8745	6.43	0.000
A-Discharge Current	1	12.689	12.6891	10.37	0.003
B-Pulse on Time	1	4.257	4.2573	3.48	0.070
C- Servo Voltage	1	13.990	13.9904	11.43	0.002
D-Con. of powder	1	1.480	1.4798	1.21	0.278
E-Tool Material	1	1.308	1.3085	1.07	0.307
F-% Reinforcement	1	4.620	4.6196	3.78	0.059
Square	4	52.436	13.1091	10.71	0.000
B*B	1	6.070	6.0697	4.96	0.032
D*D	1	38.901	38.9012	31.79	0.000
E*E	1	14.324	14.3238	11.71	0.001
F*F	1	7.010	7.0099	5.73	0.021
2-Way Interaction	3	13.656	4.5519	3.72	0.019
C*D	1	7.311	7.3115	5.97	0.019
C*F	1	3.057	3.0573	2.50	0.122
D*E	1	3.287	3.2870	2.69	0.109
Error	40	48.949	1.2237		
Lack-of-Fit	34	33.591	0.9880	0.39	0.964
Pure Error	6	15.358	2.5597		
Total	53	161.727			

A degree of confidence of 95% was employed for identifying important machining factors, including the TWR and Ra. It was concluded that tool material, powder concentration, servo voltage, discharge current, and pulse on time had the greatest impact on MRR. The pulse time, the voltage, the quantity of powder all has great impact on TWR, while the tool material has a significant impact on Ra. The high discharge energy quickly breaks down the material, therefore increasing its resistance.

## 5.2 Prediction using ANN

Analogous neural networks can be used to forecast response parameters for a given set of process parameters. To obtain the most accurate predictions the neural network should be trained with some samples before testing. The weights and bias values have been calculated as 6–15–15–3 structure To perform the ANN prediction, the network received six input

variables— $I_p$ , Ton, Vs, C, material, reinforced % and three output variables—MRR, TWR, and SR Matlab software ANN prediction module has been used to separate training data from test data. The literature has reported that training data of 70% can lead to more accurate results of prediction. The current study kept 70% of the training data for prediction, and the rest for training. ANN models produce six input parameters and three output parameters by varying the number of neurons in the hidden layer. For optimal regression values, not only the number of neurons in the hidden layer should be varied, but also the learning rate and the momentum coefficient. The learning rate should be varied between 0 and 1, while the momentum coefficient should be varied between 0 and 2.

An ANN system demonstrates the capability to handle complex functions. It has been successfully utilized in a variety of industries for multiple purposes, including defect detection, process identification, estimation of property values, smoothing of data and error detection. A neural network can also be effectively used for designing and developing products, optimizing processes and estimating activity coefficients [120, 121]. Based on the concept of biological neural networks, a neural network could be regarded as a massively parallel, highly distributed tool for processing large amount of data. It consists of a set of neurons capable of acquiring, learning and adjusting to new information to ensure that knowledge is retained [122]. A multi-layered neural network was used to simulate the SCMEDM process and predict the TWR, MRR and Ra response variables for the machining of aluminium and SiC MMC.

### 5.3 ANN Performance

A total of fifty-four unique input–output patterns were analysed using the NN package in MATLAB. The assumption

$X=N_1-N_2-Y$  is used for generalised ANN models. Where X, represents the input layer's number of neurons,  $N_1$  denotes the first hidden layer's number of neurons,  $N_2$  denotes the second hidden layer's number of neurons and Y denotes the output layer's number of neurons. In addition, noise was included in the weights to help keep the network structure stable whilst it was tuned for performance. The model was trained using a technique known as Levenberg–Marquardt (LM), which is a kind of optimization algorithm. The following Eq. (3) was used to evaluate the network's performance using the Mean Square Error (MSE).

$$MSE = \frac{1}{M \times N} \sum_{j=1}^N \sum_{i=1}^N (Y'_i - Y_i)^2 \quad (3)$$

$Y_i$  signifies the  $i$ th neuron's experimental output,  $Y'_i$  signifies the  $i$ th neuron's projected output, N signifies the total number of training patterns and M signifies the total number of neurons in the output layer [123]. There have been numerous optimization efforts made by altering the number of neurons in the first layer of the 6- $N_1$ -15-3 NN. The number of neurons in the  $N_1$  layer was fixed at fifteen while the number of neurons in the second hidden layer was varied between one and fifteen to improve the 6-15- $N_2$ -3 algorithm. With this approach, the total number of neuron combinations in the hidden layers could be significantly reduced. The ANN model is trained using 38 of the 54 experimental values and the trained ANN model is tested using 16 of the 54 experimental values. Variation in the mean squared error during ANN model training for various epoch counts was investigated. At epoch 5, the best validation was seen with an MSE of 2.086 in the single hidden layer (Fig. 2). The regression coefficient acquired during the training of the ANN model is 0.99657, which is extremely close to one. The best validation performance value achieved using a double hidden layer is 2.9188 at epoch 3, as shown in Fig. 3 and the

**Fig. 2** Experimental and predicted MRR value

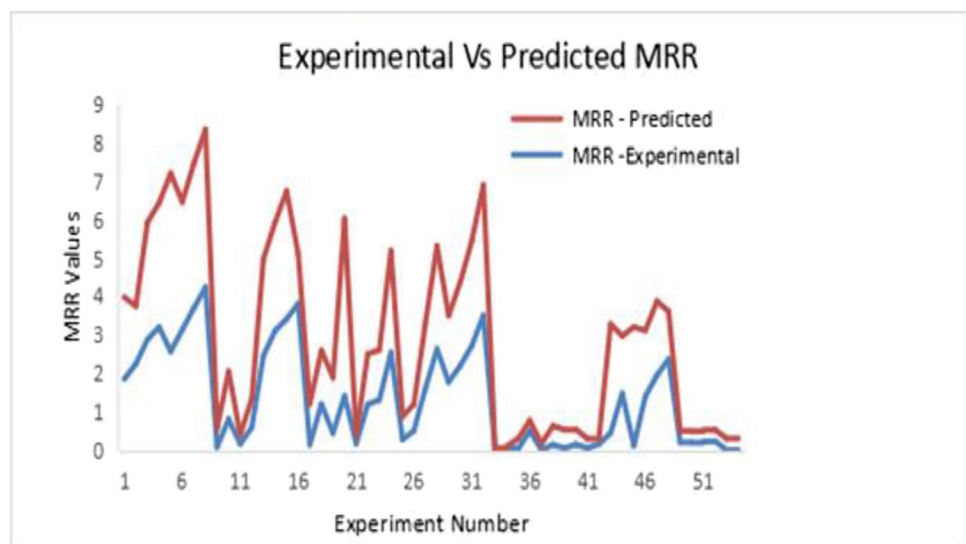
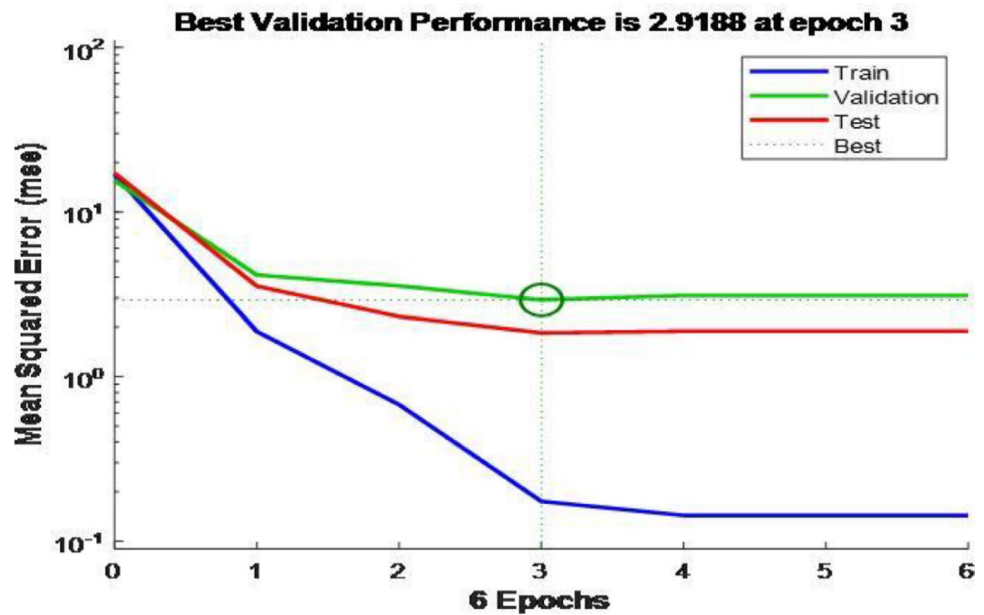


**Fig. 3** Mean squared errors obtained during ANN training (double hidden layer)



corresponding experimental and predicted values for TWR as a sample are depicted in Fig. 2. The regression coefficient acquired during the training of the ANN model was 0.99308. To prevent local minima, the NN structure was trained several times with negligible weight variation throughout the training phase. Thus, in the study, the 6–15–15–3 (Double hidden layer) structure was used to evaluate the performance of SCMEDM processes (Table 7).

#### 5.4 A Parametric Study on Machine Response Using the RSM Model

The new ANN model 6–15–15–3 (double hidden layer) was used to test the influence of input process parameters on response variables. While graphs for each parameter were constructed, the rest were left at their default values of 0.

##### 5.4.1 Parametric effect on MRR

Based on their results in Table 4, the following parameters also have a significant effect on MRR:  $I_p$ ,  $T_{on}$ ,  $V_s$ ,  $C$ , tool material, and % reinforcement. However,  $I_p$  is the most influencing parameter, showing a sharp spike in MRR by 2.4 mm<sup>3</sup>/min when it decreases initially before increasing from 3 to 4A. The reason for this is that an increase in peak current produces more heat energy and hence increases the melting and evaporation of material from the workpiece, resulting in an increased MRR. In addition, the MRR increases by 1.2 mm<sup>3</sup>/min when  $T_{on}$  is raised from 30 to 75 s, and it increases by even more when the servo voltage is raised from 50 to 70 V. The voltage has become increasingly dominant in MRR because of a decrease in electrode gap between the workpiece and the tool. By adding large amounts of abrasive

particles to dielectric liquid the dielectric strength of the fluid is enhanced as well, which raises the MRR. As a result of their high thermal conductivity, copper tools produce a higher MRR than brass and graphite tools and the addition of 1% reinforcement to a workpiece has the least impact on MRR (46%) (Fig. 4).

##### 5.4.2 Parametric effect on TWR

Furthermore, the TWR was graphically analyzed with input parameters and  $I_p$ ,  $T_{on}$ ,  $V_s$  and  $C$  was found to have significant impacts on the TWR, as shown in Table 6. The most influential parameter,  $I_p$ , indicates significant increases in TWR when the current increases steeply from 2 to 4A. Also, the mean TWR increases directly proportional to the  $T_{on}$  when the  $T_{on}$  increases the time from 52.5 s to 75 s. In addition, TWR increases with an increase in servo voltage from 50 to 70 v. In fact, abrasive particles in the dielectric liquid appear to be the main factor affecting the TWR. This indicates that powder concentration is the most important factor for the TWR. The tool material also has a considerable impact on the tool wear rate. Despite the fact that 100% reinforcement was found insignificant in the current study, its effect cannot be ignored when compared to other parameters [124] (Fig. 5).

##### 5.4.3 The Parametric Influence on SR

From the perspective of quality, surface quality is the most important factor. Hence, the impact of input parameters on the SR was analyzed graphically, and it was discovered that  $R_a$  was maximum at a higher value of  $I_p$ ,  $T_{on}$ ,  $V_s$ , and  $C$ , and minimum at a low value, as shown in Table 6.

**Table 7** Testing the capability of ANN models using Double hidden layer for prediction of MRR, TWR and SR

S.N	Process parameter						Target values			ANN Predicted values			ANN Absolute Error		
	Ip	Ton	V	C	T	W	MRR	TWR	SR	MRR	TWR	SR	MRR	TWR	SR
	Amp	$\mu$ s	volt	gm/ltr			(mm <sup>3</sup> /min)	(mm <sup>3</sup> /min)	( $\mu$ m)	(mm <sup>3</sup> /min)	(mm <sup>3</sup> /min)	( $\mu$ m)	(mm <sup>3</sup> /min)	(mm <sup>3</sup> /min)	( $\mu$ m)
1	2	30	60	0	0	5	1.86567	0.0334	5.104	1.7399	3.0116	7.9758	0.1257	2.9781	2.8718
2	4	30	60	0	0	5	2.25835	1.8464	9.723	2.3304	1.71758	9.5503	0.0720	0.1288	0.1726
3	2	75	60	0	0	5	2.89164	2.1111	8.535	2.8058	2.1653	8.1780	0.0857	0.0541	0.3569
4	4	75	60	0	0	5	3.21343	3.5033	9.677	2.8771	3.2243	9.4535	0.3362	0.2789	0.2234
5	2	30	60	4	0	5	2.582	3.0906	9.967	1.9466	0.9014	6.2024	0.6353	2.1891	3.7645
6	4	30	60	4	0	5	3.14328	3.5928	9.885	3.2880	3.6716	9.8524	0.1447	0.0788	0.0325
7	2	75	60	4	0	5	3.71194	3.9669	9.456	3.6173	3.8431	9.5094	0.0946	0.1237	0.0534
8	4	75	60	4	0	5	4.24119	4.7223	10.646	3.4430	3.1944	11.318	0.7981	1.5278	0.6725
9	3	30	50	2	-1	5	0.10925	1.5458	7.592	0.7082	1.2536	7.0936	0.817451	0.2921	0.4983
10	3	75	50	2	-1	5	0.82119	2.9229	8.607	0.8564	2.8741	8.550	0.0352	0.0487	0.0564
11	3	30	70	2	-1	5	0.18462	2.5629	7.757	0.2842	2.6327	7.6472	0.0996	0.0698	0.1097
12	3	75	70	2	-1	5	0.61819	3.1343	8.839	1.2673	1.8115	10.092	0.6491	1.3227	1.2533
13	3	30	50	2	1	5	2.46865	2.8584	6.394	2.7390	3.0364	6.7010	0.2704	0.1780	0.3070
14	3	75	50	2	1	5	3.11925	3.6761	9.885	2.4138	0.8244	8.2218	0.705438	2.8516	1.6631
15	3	30	70	2	1	5	3.4258	3.8699	9.044	3.3744	3.8044	8.8657	0.0513	0.0654	0.1782
16	3	75	70	2	1	5	3.8225	4.5699	9.742	3.9893	4.4866	9.1413	0.1668	0.0832	0.6006
17	3	50	50	0	0	0	0.16656	2.6334	6.583	0.3141	2.2205	6.7696	0.1475	0.4129	0.1866
18	3	50	70	0	0	0	1.20894	2.9223	9.884	1.1904	2.9778	9.5585	0.0184	0.0555	0.3254
19	3	50	50	4	0	0	0.46776	3.0446	10.832	0.8355	1.3340	9.3629	0.3678	1.7105	1.4690
20	3	50	70	4	0	0	1.42314	3.8558	9.847	1.2937	3.6094	9.937	0.1293	0.2463	0.0901
21	3	50	50	0	0	10	0.1985	0.7334	6.499	0.6225	0.5410	6.6001	0.4240	0.1923	0.1011
22	3	50	70	0	0	10	1.20297	1.5111	9.09	1.0652	1.4142	8.7451	0.1377	0.0968	0.3448
23	3	50	50	4	0	10	1.32313	1.5223	9.432	1.3761	1.3994	9.2243	0.0529	0.1228	0.2076
24	3	50	70	4	0	10	2.55119	1.8446	8.661	2.7055	1.9121	8.5628	0.1543	0.0674	0.0981
25	2	50	60	0	-1	5	0.30144	1.0229	9.278	0.8882	0.9658	7.5153	0.5868	0.0570	1.7626
26	4	50	60	0	-1	5	0.52388	2.5436	9.849	0.5048	2.5747	9.6749	0.0190	0.0403	0.1741
27	2	50	60	4	-1	5	1.61731	1.378	7.142	1.6037	1.1876	7.2296	0.0135	0.1903	0.0876
28	4	50	60	4	-1	5	2.64328	1.9771	9.813	1.0564	2.8280	8.1873	1.5868	0.8509	1.6256
29	2	50	60	0	1	5	1.78656	0.6327	8.697	1.7234	0.7017	8.7143	0.0631	0.0690	0.0173
30	4	50	60	0	1	5	2.20716	1.9897	9.83	2.2380	1.6848	6.8361	0.0309	0.3048	2.9938
31	2	50	60	4	1	5	2.72895	1.3716	10.851	2.1895	0.3574	6.7496	0.5394	1.0142	4.1013
32	4	50	60	4	1	5	3.51462	2.8893	10.632	3.4028	2.8093	10.568	0.1117	0.0800	0.0639
33	3	30	60	2	-1	0	0.03731	0.8229	10.337	0.0991	0.8832	10.038	0.0618	0.0603	0.289
34	3	75	60	2	-1	0	0.07626	1.8334	10.937	1.7224	3.6281	11.468	1.6461	1.7946	0.5317
35	3	30	60	2	1	0	0.05462	0.5442	8.457	0.6378	1.3047	9.0700	0.5832	0.7605	0.6130
36	3	30	60	2	1	0	0.5231	1.8097	9.557	0.6378	1.3047	9.0700	0.1147	0.5049	0.4869
37	3	30	60	2	0	10	0.03231	0.0229	7.132	0.1805	0.0705	6.9075	0.1482	0.0476	0.2244
38	3	75	60	2	-1	10	0.16119	0.8114	7.782	0.0169	0.7425	7.9358	0.1442	0.0689	0.1538
39	3	30	60	2	1	10	0.07462	0.0442	7.478	0.8934	0.6766	5.8829	0.8188	0.7209	1.5950
40	3	75	60	2	1	10	0.16925	0.7442	8.209	0.4591	0.8344	8.2009	0.2899	0.0902	0.0080
41	2	50	50	2	0	0	0.07731	0.0111	7.249	0.3579	2.0334	6.2650	0.2806	2.0222	0.9839
42	4	50	50	2	0	0	0.18119	0.2223	8.819	0.4898	0.2970	8.7608	0.3087	0.0747	0.0581
43	2	50	70	2	0	0	0.46831	0.0711	6.463	0.4055	0.1453	6.3926	0.0627	0.0742	0.0703
44	4	50	70	2	0	0	1.48656	0.0811	9.192	1.4422	0.2603	8.7464	0.0442	0.1791	0.4455
45	2	50	50	2	0	10	0.13731	0.0823	5.394	0.0744	0.3868	6.4568	0.0628	0.3044	1.0628
46	4	50	50	2	0	10	1.41656	0.0111	5.471	1.6285	-0.05842	5.9198	0.2119	0.0695	0.4488
47	2	50	70	2	0	10	1.96104	0.7223	7.946	1.9845	0.6586	7.5425	0.0234	0.0637	0.4034

**Table 7** (continued)

S.N	Process parameter						Target values			ANN Predicted values			ANN Absolute Error		
	Ip	Ton	V	C	T	W	MRR	TWR	SR	MRR	TWR	SR	MRR	TWR	SR
	Amp	μs	volt	gm/ltr			(mm <sup>3</sup> /min)	(mm <sup>3</sup> /min)	(μm)	(mm <sup>3</sup> /min)	(mm <sup>3</sup> /min)	(μm)	(mm <sup>3</sup> /min)	(mm <sup>3</sup> /min)	(μm)
48	4	50	70	2	0	10	2.38059	1.6508	9.996	2.2602	1.7261	9.8858	0.1203	0.0752	0.1101
49	3	50	60	2	0	5	0.22388	0.0446	8.153	0.2321	0.0484	5.8971	0.0082	0.0038	2.2558
50	3	50	60	2	0	5	0.21656	0.0334	4.788	0.2321	0.0484	5.8971	0.0155	0.0149	1.1091
51	3	50	60	2	0	5	0.24850	0.0111	4.711	0.2321	0.0484	5.8971	0.0163	0.0373	1.1861
52	3	50	60	2	0	5	0.25626	0.0334	4.432	0.2321	0.0484	5.8971	0.0241	0.0149	1.4651
53	3	50	60	2	0	5	0.02631	0.0111	8.13	0.2321	0.04846	5.8971	0.2058	0.0373	2.2328
54	3	50	60	2	0	5	0.01274	0.0111	6.073	0.2321	0.04846	5.8971	0.2193	0.0373	0.1758

**Fig. 4** Effect of input parameter on MRR

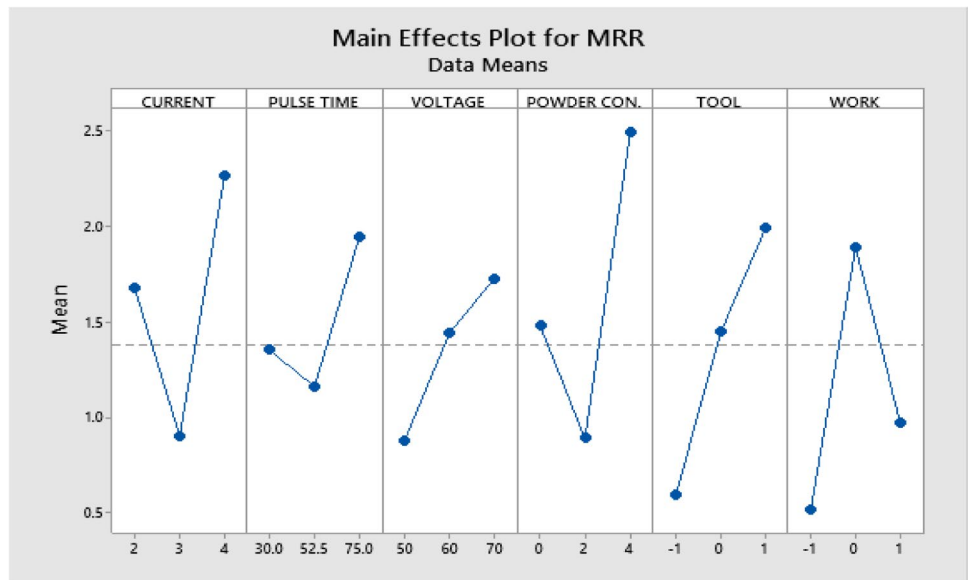
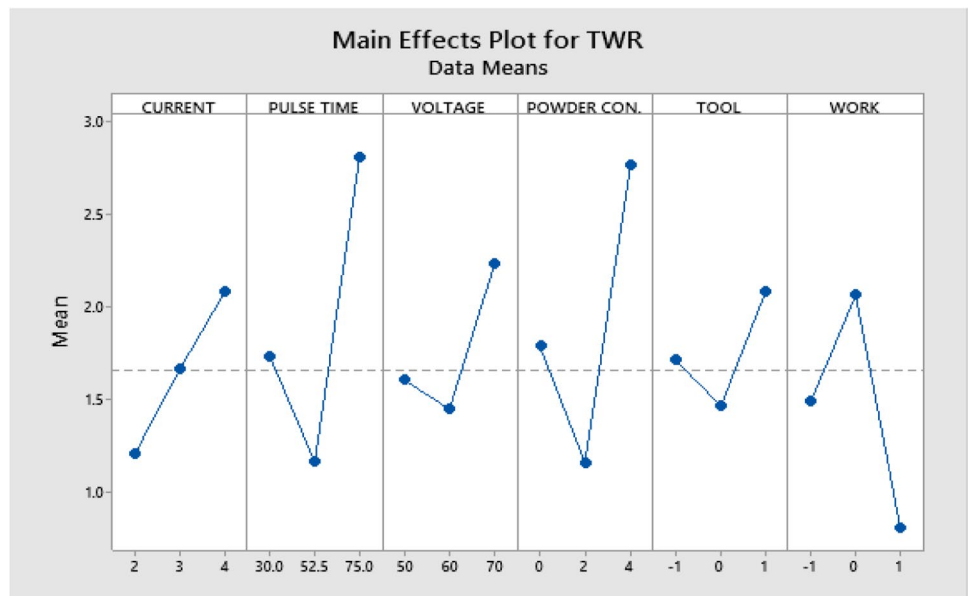


**Fig. 5** Effect of input parameter on TWR



However  $I_p$  is the most important parameter that increases Ra value with an incremental current from 2 to 4A as a result, the SR is mainly affected by current. In addition, Ra increases by  $9.5 \mu\text{m}$  when  $T_{on}$  increases from 52.5 s to 75.0 s, respectively. Additionally, Ra increased by  $9.5 \mu\text{m}$  when  $T_{on}$  increased from 52.5 s to 75.0 s, and Ra is also directly proportional to voltage for the same range of IP and V. In the present study, surface quality was also affected by the addition of abrasive particles. These particles speed up the material removal process, resulting in a decline in SR. Tool material selection also affects surface quality, as tool reinforcement has a negative impact on Ra (Fig. 6).

### 5.5 Morphology of the SEM Image

As reported in the literature, the discharge energy is responsible for the bulk of the changes in surface texture throughout the SCMEDM process. As a result, a variety of parametric settings were tested to determine the surface quality of specimens machined using SCMEDM. A material characterization reveals uneven deposition, pockmarks, holes, debris globules, as well as an appearance of a white layer. The run order of 31 specimens is shown in Fig. 7;

Despite higher MRR being obtained from the high discharge energy strike on the surface, there were still deep pockets, lower debris and a recast layer with a poor SF in the machine [125]. The discharge energy is directly proportional to the size of the crater and the amount of metal removed. Increased discharge enlarges and multiplies globules, voids and pockmarks. White layer (also known as recast layer) also undergoes thermal and chemical reactions; which can result in changes to the chemical composition of the upper layers as well as phase shifts. The white layer is often harder than

the bulk material due to its oxide content. It is important to note that the effects of SCMEDM parameters on the LM-25/SiC composite surface layers have not been examined in this study and more investigation is needed.

## 6 Conclusions

The purpose of this study is to develop a ANN model for the prediction of performance measures that include Metal Removal Rate (MRR), Tool Wear Rate (TWR) and Surface Roughness (Ra) for the SCMEDM process for machining LM-25/SiC composites and examining the significance of machining parameters such as discharge current ( $I_p$ ), pulse on-time ( $T_{ON}$ ), servo voltage, powder concentration, tool materials and percent reinforcement for performance measures.

Design of Experiments (DOE), Artificial Neural Networks (ANN) and Analysis of Variances (ANOVA) are used as models in this study. The designed ANN model accurately predicted MRR, TWR and Ra values as a result of the approach taken. As a result of the used approach, the developed ANN model was able to predict MRR, TWR and Ra values with excellent accuracy as a result of the approach adopted. During the training of the ANN model, the regression coefficient obtained is 0.99308; for validation is 0.89047 and for testing the trained ANN model is 0.94429. The overall regression coefficient is 0.96811,

This research may have both practical and theoretical ramifications. On the practical side, the results of the research can help practitioners develop an effective and efficient SCMEDM technique for machining LM-25/SiC

**Fig. 6** Effect of input parameter for SR

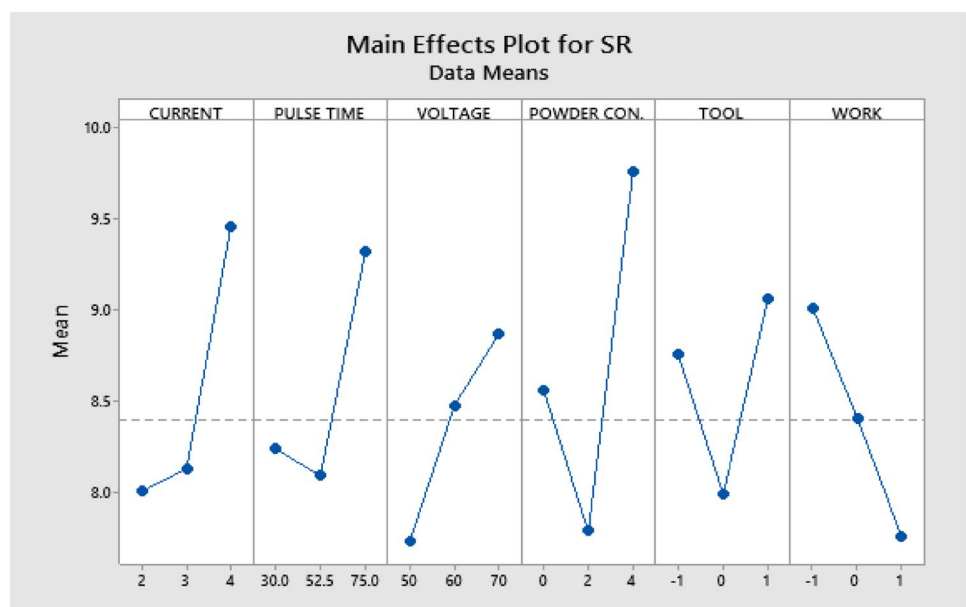
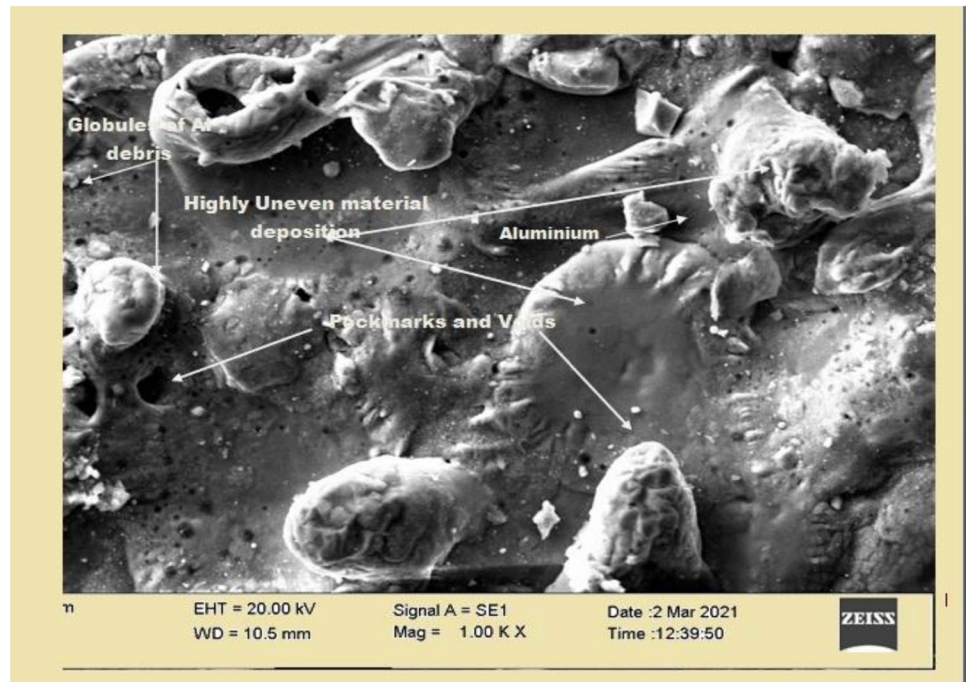


**Fig. 7** Run order-31, SEM micrograph at A=3A, B=30  $\mu$ s, C=60 V, D=2gm/ltr, E=Brass tool, F=LM-25/SiC (10%)



MMC. On the other side, theoretical implications include expanding knowledge of the SCMEDM process database and gaining a better grasp of the linkages between machining parameters and performance measurements. Future study could involve optimising the SCMEDM process for cutting different materials or the same material but with different sets of machining parameters and performance measurements. Another research strategy may be to optimise the SCMEDM process for cutting the same material but using different optimization tools and comparing the results to validate present research findings. The following conclusions have been reached as a result of this research:

1. As the results of the ANOVA analysis showed, the tool material had the largest effect on the SCMEDM machining of the LM-25/SiC composite. According to this research, the tool material is the most influential parameter for MRR, with the highest percentage of contribution of 11.90%, followed by powder concentration, servo voltage, discharge current, pulse-on-time and reinforcement, with contributions of 7.15%, 5.02%, 4.04% and 3.24%, respectively.
2. In ANOVA analysis, the predictive error for the RSM models for MRR, TWR and Ra is less than 6% on average for experimental values.
3. By employing a feed-forward back propagation neural network with a 6–15–15–3 structure, it was possible to generate an accurate process model. The best validation

performance value was 2.9188 at epoch 3 when using a double hidden layer.

4. By comparing the results predicted by ANN models and RSM models, it was found that ANN generated more reliable and acceptable results for the study than RSM because of its higher modeling capability.
5. Compared to the RSM model, the neural network model forecasts MRR, TWR and Ra better. The decrease predicted value of the neural network model compares favorably to that of the RSM model.
6. In high discharge energy settings, SCMEDM-machined materials produced larger debris globules, more pockmarks and more uneven layer deposition.

**Authors' Contributions** Samples preparation, data collection and analysis were performed by the authors SST and SKP. The first draft of the manuscript was written by SST. SS and KKS contributed during editing and revision work of the paper. All authors commented on previous versions of the manuscript. All authors read and approved the final manuscript.

**Funding** This work did not receive a financial support.

**Data Availability** The data and material are available within the manuscript.

**Code Availability** Not applicable.

The authors declare that all procedures followed were in accordance with the ethical standards.

## Declarations

**Conflict of Interest** The authors declare that there is no conflict of interest regarding the publication of this paper.

**Consent to Participate** All the authors declare their consent to participate in this research article.

**Consent for Publication** All the authors declare their consent for publication of the article on acceptance.

**Competing Interests** The authors have no relevant financial or non-financial interests to disclose.

## References

- Gopalakannan S, Senthilvelan T, Kalaichelvan K (2012) Modeling and optimization of EDM process parameters on machining of Al 7075/SiC metal matrix composites by applying response surface method. *J Mech Eng* 63(1):37–51
- Venkatesan K (2017) The study on force, surface integrity, tool life and chip on laser assisted machining of inconel 718 using Nd: YAG laser source. *J Adv Res* 8(4):407–423
- Gopalakannan S, Senthilvelan T, Kalaichelvan K (2012) Modeling and optimization of Al 7075/10wt% Al<sub>2</sub>O<sub>3</sub> metal matrix composites by response surface method. *Adv Mater Res* 488–489:856–860
- Kaczmar JW, Pietrzak K, Wlosinski W (2000) The production and application of metal matrix composites material. *J Mater Process Technol* 106:58–67
- Sleziona J (1995) Influence ceramic particles on Al–SiC, Al–Al<sub>2</sub>O<sub>3</sub> composites solidification. *Arch Mater Sci* 16:163–178
- Chiang K-T, Chang F-P, Tsai D-C (2007) Modeling and analysis of the rapidly resolidified layer of SG cast iron in the EDM process through the response surface methodology. *J Mater Process Technol* 182(1–3):525–533
- Habib SS (2009) Study of the parameters in electrical discharge machining through response surface methodology approach. *Appl Math Model* 33(12):4397–4407
- Prabhu S, Uma M, Vinayagam BK (2013) Electrical discharge machining parameters optimization using response surface methodology and fuzzy logic modeling. *J Braz Soc Mech Sci Eng* 36(3):637–652
- Hourmand M, Farahany S, Sarhan AAD, Noordin MY (2014) Investigating the electrical discharge machining (EDM) parameter effects on Al-Mg2Si metal matrix composite (MMC) for high material removal rate (MRR) and less EWR–RSM approach. *Int J Adv Manuf Technol* 77(5–8):831–838
- Barenji RV, Pourasl HH, Khojastehnezhad VM (2016) Electrical discharge machining of the AISI D6 tool steel: prediction and modeling of the material removal rate and tool wear ratio. *Precis Eng* 45:435–444
- Soundhar A, Zubar HA, Sultan MTBH, Kandasamy J (2019) Dataset on optimization of EDM machining parameters by using central composite design. *Data Brief* 23:103671
- Mandal D, Pal SK, Saha P (2007) Modeling of electrical discharge machining process using back propagation neural network and multi-objective optimization using non-dominating sorting genetic algorithm-II. *J Mater Process Technol* 186(1–3):154–162
- Markopoulos AP, Manolakos DE, Vaxevanidis NM (2008) artificial neural network models for the prediction of surface roughness in electrical discharge machining. *J IntellManuf* 19(3):283–292
- Pradhan MK, Das R, Biswas CK (2009) Comparisons of neural network models on surface roughness in electrical discharge machining. *Proc Inst Mech Eng B J EngManuf* 223(7):801–808
- Sidhu SS, Batish A, Kumar S (2013) Neural network–based modeling to predict residual stresses during electric discharge machining of Al/SiC metal matrix composites. *Proc Inst Mech Eng B J EngManuf* 227(11):1679–1692
- Kumar S, Batish A, Singh R, Singh TP (2014) A hybrid Taguchi-artificial neural network approach to predict surface roughness during electric discharge machining of titanium alloys. *J Mech Sci Technol* 28(7):2831–2844
- Ong P, Chong CH, Bin Rahim MZ, Lee WK, Sia CK, Bin Ahmad MAH (2018) Intelligent approach for process modeling and optimization on electrical discharge machining of polycrystalline diamond. *J Intell Manuf* 31(227):247
- Lin M, Tsao C, Hsu C, Chiou A, Huang P, Lin Y (2013) Optimization of micro milling electrical discharge machining of Inconel 718 by Grey-Taguchi method. *Trans Nonferrous Metals Soc China* 23(3):661–666
- Nikalje AM, Kumar A, Srinadh KVS (2013) Influence of parameters and optimization of EDM performance measures on MDN 300 steel using Taguchi method. *Int J Adv Manuf Technol* 69(1–4):41–49
- Tang L, Guo YF (2013) Electrical discharge precision machining parameters optimization investigation on S-03 special stainless steel. *Int J Adv Manuf Technol* 70(5–8):1369–1376
- Gaikwad V, Jatti VS (2018) Optimization of material removal rate during electrical discharge machining of cryo-treated NiTi alloys using Taguchi's method. *J King Saud Univ - Eng Sci* 30(3):266–272
- Jung JH, Kwon WT (2010) Optimization of EDM process for multiple performance characteristics using Taguchi method and Grey relational analysis. *J Mech Sci Technol* 24(5):1083–1090
- Singh S (2012) Optimization of machining characteristics in electric discharge machining of 6061Al/Al<sub>2</sub>O<sub>3</sub>p/20P composites by grey relational analysis. *Int J Adv Manuf Technol* 63(9–12):1191–1202
- Yadav US, Yadava V (2014) Experimental modeling and multiobjective optimization of electrical discharge drilling of aerospace superalloy material. *Proc Inst Mech Eng B J EngManuf* 229(10):1764–1780
- Khanna R, Kumar A, Garg MP, Singh A, Sharma N (2015) Multiple performance characteristics optimization for Al 7075 on electric discharge drilling by Taguchi grey relational theory. *J Indust Eng Int* 11(4):459–472
- Selvarajan L, Manohar M, Udhayakumar A, Dhinakaran P (2017) Modelling and experimental investigation of process parameters in EDM of Si<sub>3</sub>N<sub>4</sub>-TiN composites using GRARSM. *J Mech Sci Technol* 31(1):111–122
- Tzeng C-J, Chen R-Y (2013) Optimization of electric discharge machining process using the response surface methodology and genetic algorithm approach. *Int J Precis EngManuf* 14(5):709–717
- Gopalakannan S, Senthilvelan T (2013) Application of response surface method on machining of Al–SiC nano-composites. *Measurement* 46(8):2705–2715
- Hegab HA, Gadallah MH, Esawi AK (2015) Modeling and optimization of electrical discharge machining (EDM) using statistical design. *Manuf Rev* 2:21
- Swiercz R, Oniszczuk-Świercz D, Chmielewski T (2019) Multiresponse optimization of electrical discharge machining using the desirability function. *Micromachines* 10(1):72
- Jagadish, & Ray, A. (2015) Optimization of process parameters of green electrical discharge machining using principal component analysis (PCA). *Int J Adv Manuf Technol* 87(5–8):1299–1311



32. Sahu SN, Nayak NC (2018) Multi-criteria decision making with PCA in EDM of A2 tool steel. *Mater Today: Proc* 5(9):18641–18648
33. Routara BC, Bhuyan RK, Parida AK (2014) Application of the entropy weight and TOPSIS method on Al–12% SiC metal matrix composite during EDM. *Int J Manuf, Mater Mech Eng* 4(4):49–63
34. Dewangan S, Gangopadhyay S, Biswas CK (2015) Study of surface integrity and dimensional accuracy in EDM using fuzzy TOPSIS and sensitivity analysis. *Measurement* 63:364–376
35. Tripathy S, Tripathy DK (2016) Multi-attribute optimization of machining process parameters in powder mixed electro-discharge machining using TOPSIS and grey relational analysis. *Eng Sci Technol Int J* 19(1):62–70
36. Padhee S, Nayak N, Panda SK, Dhal PR, Mahapatra SS (2012) Multi-objective parametric optimization of powder mixed electro-discharge machining using response surface methodology and nondominated sorting genetic algorithm. *Sadhana* 37(2):223–240
37. Bharti PS, Maheshwari S, Sharma C (2012) Multi-objective optimization of electric-discharge machining process using controlled elitist NSGA-II. *J Mech Sci Technol* 26(6):1875–1883
38. Baraskar SS, Banwait SS, Laroiya SC (2013) Multiobjective optimization of electrical discharge machining process using a hybrid method. *Mater Manuf Process* 28(4):348–354
39. Sharma N, Singh G, Gupta MK, Hegab H, Mia M (2019) Investigations of surface integrity, bio-activity and performance characteristics during wire- electrical discharge machining of Ti- 6Al-7Nb biomedical alloy. *Mater Res Exp* 6(9):1–16
40. Majumder A, Das PK, Majumder A, Debnath M (2014) An approach to optimize the EDM process parameters using desirability-based multi-objective PSO. *Prod Manuf Res* 2(1):228–240
41. Mohanty CP, Mahapatra SS, Singh MR (2014) A particle swarm approach for multi-objective optimization of electrical discharge machining process. *J IntellManuf* 27(6):1171–1190
42. Dey A, Debnath M, Pandey KM (2017) Analysis of effect of machining parameters during electrical discharge machining using Taguchi-based multi-objective PSO. *Int J ComputIntell Appl* 16(02):1750010
43. Moghaddam MA, Kolahan F (2019) Using combined artificial neural network and particle swarm optimization algorithm for modeling and optimization of electrical discharge machining process. *Sci Iran*
44. Yildiz Y, Sundaram MM, Rajurkar KP (2012) Statistical analysis and optimization study on the machinability of beryllium–copper alloy in electro discharge machining. *Proc Inst Mech Eng B J EngManuf* 226(11):1847–1861
45. Muthuramalingam T, Mohan B (2013) Influence of discharge current pulse on machinability in electrical discharge machining. *Mater Manuf Process* 28(4):375–380
46. Torres A, Puertas I, Luis CJ (2015) EDM machinability and surface roughness analysis of INCONEL 600 using graphite electrodes. *Int J Adv Manuf Technol* 84(9–12):2671–2688
47. Rahul D, S., Biswal, B. B., & Mahapatra, S. S. (2019) Machinability analysis of Inconel 601, 625, 718 and 825 during electro-discharge machining: on evaluation of optimal parameters setting. *Measurement* 137:382–400
48. Nalbant M, Altın A, Gökkaya H (2007) The effect of cutting speed and cutting tool geometry on machinability properties of nickel-base Inconel 718 super alloys. *Mater Des* 28(4):1334–1338
49. Chalisgaonkar R, Kumar J (2015) Multi-response optimization and modeling of trim cut WEDM operation of commercially pure titanium (CPTi) considering multiple user's preferences. *Eng Sci Technol Int J* 18(2):125–134
50. Sharma N, Khanna R, Gupta RD (2015) WEDM process variables investigation for HSLA by response surface methodology and genetic algorithm. *Eng Sci Technol Int J* 18(2):171–177
51. Shrivastava PK, Dubey AK (2013) Experimental modeling and optimization of electric discharge diamond face grinding of metal matrix composite. *Int J Adv Manuf Technol* 69(9–12):2471–2480
52. Rajesh R, DevAnand M (2016) Prediction of EDM process parameters for a composite material using RBFNN and ANN through RSM. *Indian J Sci Technol* 9:1–12
53. Surya VR, Kumar KV, Keshavamurthy R, Ugrasen G, Ravindra HV (2017) Prediction of machining characteristics using artificial neural network in wire EDM of Al7075 based in-situ composite. *Mater Today: Proc* 4(2):203–212
54. Dubey V, Sharma AK, Singh B (2022) Optimization of machining parameters in chromium-additive mixed electrical discharge machining of the AA7075/5% B4C composite. *Proc IME E J Process Mech Eng* 236(1):104–113
55. Phate MR, Toney SB, Phate VR (2021) Multi-parametric optimization of WEDM using artificial neural network (ANN)-based PCA for Al/SiCp MMC. *J Inst Eng (India): Ser C* 102(1):169–181
56. Preetham NS, Muniappan A, Jayakumar KS, Maridurai T (2021) Experimental investigation of machining conditions on Surface Roughness in WEDM of Aluminum hybrid composite by RSM. *Mater Today: Proc*
57. Thakur SS, Patel B, Upadhyay RK (2021) Soft computing technique based modelling of ceramics mix electric discharge machining on LM-25/SiC composites. *Mater Today: Proc*
58. Singh NK, Singh Y, Kumar S, Sharma A (2019) Comparative study of statistical and soft computing-based predictive models for material removal rate and surface roughness during helium-assisted EDM of D3 die steel. *SN Appl Sci* 1(6):1–12
59. Agrawal A, Dubey AK, Shrivastava PK (2013) Modeling and optimization of tool wear rate in powder mixed EDM of MMC. In 2nd International Conference on Mechanical and Robotics Engineering (ICMRE'2013) Dec (pp. 17–18)
60. Kumar R, Chauhan S (2015) Study on surface roughness measurement for turning of Al 7075/10/SiCp and Al 7075 hybrid composites by using response surface methodology (RSM) and artificial neural networking (ANN). *Measurement* 65:166–180
61. Bhuyan RK, Mohanty S, Routara BC (2017) RSM and Fuzzy logic approaches for predicting the surface roughness during EDM of Al-SiCp MMC. *Mater Today: Proc* 4(2):1947–1956
62. Kumar KR, Sreebalaj VS (2017) Artificial Neural Networks based prediction and Multi Response Optimization on EDM of Aluminium/Fly ash composites. *Int J Theor Appl Mech* 2
63. Unune DR, Barzani MM, Mohite SS, Mali HS (2018) Fuzzy logic-based model for predicting material removal rate and average surface roughness of machined Nimonic 80A using abrasive-mixed electro-discharge diamond surface grinding. *Neural Comput Appl* 29(9):647–662
64. Sahu SK, Naik S, Das SR, Dhupal D (2019) Parametric optimization of surface roughness and overcut in electric discharge machining of Al-SiC using copper electrode. In *Renewable Energy and its Innovative Technologies* (pp. 99–116). Springer, Singapore
65. Ubale SB, Deshmukh SD, Ghosh S (2018) Artificial Neural Network based Modelling of Wire Electrical Discharge Machining on Tungsten-Copper Composite. *Mater Today: Proc* 5(2):5655–5663
66. Lalwani V, Sharma P, Pruncu CI, Unune DR (2020) Response surface methodology and artificial neural network-based models for predicting performance of wire electrical discharge machining of inconel 718 alloy. *J Manuf Mater Process* 4(2):44
67. Manikandan N, Balasubramanian K, Palanisamy D, Gopal PM, Arulkirubakaran D, Binoj JS (2019) Machinability analysis

- and ANFIS modelling on advanced machining of hybrid metal matrix composites for aerospace applications. *Mater Manuf Process* 34(16):1866–1881
68. Singh M, Maharana S, Yadav A, Singh R, Maharana P, Nguyen TV, Yadav S, Loganathan MK (2021) An experimental investigation on the material removal rate and surface roughness of a hybrid aluminum metal matrix composite (Al6061/sic/gr). *Metals* 11(9):1449
  69. Phate M, Toney S, Phate V (2020) Modelling and investigating the impact of EDM parameters on surface roughness in EDM of Al/Cu/Ni Alloy. *Aust J Mech Eng* 1–14
  70. Tripathy S, Tripathy DK (2017) Multi-response optimization of machining process parameters for powder mixed electro-discharge machining of H-11 die steel using grey relational analysis and topsis. *Mach Sci Technol* 21(3):362–384
  71. Mohanty S, Mishra A, Nanda BK, Routara BC (2018) Multi-objective parametric optimization of nano powder mixed electrical discharge machining of AlSiCp using response surface methodology and particle swarm optimization. *Alex Eng J* 57(2):609–619
  72. Reddy G, Bharath, Vamsi VSP (2015) Parametric Analysis on Powder Mixed Electric Discharge Machining Of Various Steels Using Taguchi Method. *Int J Adv Res Sci Eng IJARSE* 4(02):422
  73. Tripathy S, Tripathy DK (2016) Multi-attribute optimization of machining process parameters in powder mixed electro-discharge machining using TOPSIS and grey relational analysis, *Engineering Science and Technology. An Int J* 19:62–70
  74. Razak MA, Abdul-Rani AM, Nanimina AM (2015) Improving EDM efficiency with silicon carbide powder-mixed dielectric fluid. *Int J Mater Mech Manuf* 3(1):40–43
  75. Shabgard M, Khosrozadeh B (2017) Investigation of carbon nanotube added dielectric on the surface characteristics and machining performance of Ti–6Al–4V alloy in EDM process. *J Manuf Process* 25:212–219
  76. Kumar S, Singh R (2010) Investigating surface properties of OHNS die steel after electrical discharge machining with manganese powder mixed in the dielectric. *Int J Adv Manuf Technol* 50(5):625–633
  77. Dubey Vineet, Singh Balbir (2018) Study of Material Removal Rate in Powder Mixed EDM of AA7075/B4C Composite. *Mater Today: Proc* 5:7466
  78. Kumar, Mathan P, Jayakumar N (2018) Surface Modification on OHNS Steel Using Cu-CrB2 Green Compact Electrode in EDM. *Mater Today: Proc* 5(9):17389–17395
  79. Surekha B, Rao PG, Bijetha B, Sai VS (2018) Surface characteristics of EN19 steel materials by EDM using Graphite mixed Dielectric medium. *Mater Today: Proc* 5(9):17895–17900
  80. Roy C, Syed KH, Kuppan P (2016) Machinability Of Al/10%SiC/ 2.5%TiB2 Metal Matrix Composite With Powder-Mixed Electrical Discharge Machining. *Proc Technol* 25:1056–1063
  81. Bai X et al (2013) Machining efficiency of powder mixed near dry electrical discharge machining based on different material combinations of tool electrode and workpiece electrode. *J Manuf Process* 15(4):474–482
  82. Talla G, Gangopadhyay S, Biswas CK (2014) Multi response optimization of powder mixed electric discharge machining of aluminum/alumina metal matrix composite using grey relation analysis. *Proc Mater Sci* 5:1633–1639
  83. Kumar H (2015) Development of mirror like surface characteristics using nano powder mixed electric discharge machining (NP/EDM). *Int J Adv Manuf Technol* 76(1):105–113
  84. Toshimitsu R, Okada A, Kitada R, Okamoto Y (2016) Improvement in surface characteristics by EDM with chromium powder mixed fluid. *Proc Cirp* 42:231–235
  85. Bajaj R, Tiwari AK, Dixit AR (2015) Current trends in electric discharge machining using micro and nano powder materials-A Review. *Mater Today: Proc* 2(4–5):3302–3307
  86. Tripathy S, Tripathy DK (2017) An approach for increasing the micro-hardness in electrical discharge machining by adding conductive powder to the dielectric. *Mater Today: Proc* 4(2):1215–1224
  87. Al-Khazraji A, Amin SA, Ali SM (2016) The effect of SiC powder mixing electrical discharge machining on white layer thickness, heat flux and fatigue life of AISI D2 die steel. *Eng Sci Technol Int J* 19(3):1400–1415
  88. Thakur SS, Patel B, Upadhyay RK (2022) Soft computing technique based modelling of ceramics mix electric discharge machining on LM-25/SiC composites. *Mater Today: Proc* 50:2455–2461
  89. Naik S, Sabat S, Das SR, Dhupal D, Nanda BK (2021) Experimental Investigation, Parametric Optimization, and Cost Analysis in EDM of Aluminium-Silicon Carbide Metal Matrix Composite. In *Advanced Manufacturing Systems and Innovative Product Design*, pp. 175–187. Springer, Singapore
  90. Phate, Mangesh R., Shraddha B. Toney, and Vikas R. Phate (2021) Multi-parametric optimization of WEDM using artificial neural network (ANN)-based PCA for Al/SiCp MMC. *J Inst Eng (India): Ser* 102(1):169–181
  91. Ming W, Ma J, Zhang Z, Huang H, Shen D, Zhang G, Huang Yu (2016) Soft computing models and intelligent optimization system in electro-discharge machining of SiC/Al composites. *Int J Adv Manuf Technol* 87(1):201–217
  92. Padhee S, Nayak N, Panda SK, Dhal PR, Mahapatra SS (2012) Multi-objective parametric optimization of powder mixed electro-discharge machining using response surface methodology and non-dominated sorting genetic algorithm. *Sadhana* 37(2):223–240
  93. Talla G, Sahoo DK, Gangopadhyay S, Biswas CK (2015) Modeling and multi-objective optimization of powder mixed electric discharge machining process of aluminum/alumina metal matrix composite. *Eng Sci Technol Int J* 18:369–373
  94. Kolli M, Kumar A (2015) Effect of dielectric fluid with surfactant and graphite powder on Electrical Discharge Machining of titanium alloy using Taguchi method. *Eng Sci Technol Int J* 18:524–535
  95. Kansal HK, Singh S, Kumar P (2007) Effect of silicon powder mixed EDM on machining rate of AISI D2 die steel. *J Manuf Process* 9:13–22
  96. Singh S, Yeh MF (2012) Optimization of abrasive powder mixed EDM of aluminum matrix composites with multiple responses using Gray relational analysis. *J Mater Eng Perform* 21:481–491
  97. Kumar H, Davim JP (2011) Role of powder in the machining of Al/10%SiCp metal matrix composites by powder mixed electric discharge machining. *J Compos Mater* 45:133
  98. Ming QH, He LYY (1995) Powder-Suspension Dielectric Fluid for EDM. *J Mater Process Technol* 52:44–54
  99. Narumiya H, Mohri N, Saito N, Otake H, Tsunekawa Y, Takawashi T, Kobayashi K (2015) EDM by Powder Suspended Working Fluid. In *Proceedings of the 9th International Symposium for Electrical Machining, Bucharest, Romania*, pp. 207–210
  100. Özerkan B, Çoğun C (2005) Effect of Powder Mixed Dielectric on Machining Performance in Electric Discharge Machining (EDM). *GUU J Sci* 18:211–228
  101. Tzeng YF, Lee CY (2001) Effects of Powder Characteristics on Electro-Discharge Machining Efficiency. *Int J Adv Manuf Technol* 17:586–592
  102. Chow H-M, Yan BH, Huang FY, Hung JC (2000) Study of Added Powder in Kerosene for the Micro-slit Machining of Titanium Alloy using Electro-discharge Machining. *J Mater Processing Technol* 101:95103

103. Uno Y, Okada A, Hayashi Y, Tabuchi Y (1998) Surface Modification by EDM with Nickel Powder Mixed Fluid. *Int J Electr Mach* 4:4752
104. Tripathy S, Tripathy DK (2016) Multi-attribute optimization of machining process parameters in powder mixed electro-discharge machining using TOPSIS and grey relational analysis. *Engineering Science and Technology. Int J* 19(1):62–70
105. Prakash C, Kansal HK, Pabla BS, Puria S (2017) on the influence of nanoporous layer fabricated by PMEDM on  $\beta$ -Ti implant: biological and computational evaluation of bone- implant interface. *Proc Mater Today* 4(2):2298–2307. Part A
106. S. Tripathy, D.K. Tripathy (2017) An approach for increasing the micro-hardness in electrical discharge machining by adding conductive powder to the dielectric, *Proc Mater Today* 4(2):1215–1224. Part A
107. Abdul-Rani AM, Nanimina AM, Ginta TL, Razaka MA (2017) Machined surface quality in nano aluminum mixed electrical discharge machining. *Procedia Manuf* 7:510–517
108. Öpöz TT, Yaşar H, Ekmekci N, Ekmekci B (2018) Particle migration and surface modification on Ti6Al4V in SiC powder mixed electrical discharge machining. *J Manuf Process* 31:744–758
109. Kumar V, Amit K, Kumar S, Singh NK (2018) Comparative study of powder mixed EDM and conventional EDM using response surface methodology. *Proc Mater Today* 5(9):18089–18094. Part 3
110. Selvarajan L, Rajavel J, Prabakaran V, Sivakumar B, Jeeva G (2018) A review paper on EDM parameter of composite material and industrial demand material machining. *Proc Mater Today* 5(2):5506–5513. Part 1
111. Choudhury SD, Sahari NJ, Surekha B, Mondal G (2018) Study on the influence of hybridized powder mixed dielectric in electric discharge machining of alloy steels. *Proc Mater Today* 5(9):18410–18415. Part 3
112. Surekha B, Lakshmi TS, Jena H, Samal P (2019) Response surface modelling and application of fuzzy grey relational analysis to optimize the multi-response characteristics of EN-19 machined using powder mixed EDM. *Aust J Mech Eng (Print)* 2204–2253
113. Kasman Ş, Saklakoglu IE (2012) Determination of process parameters in the laser micromilling application using Taguchi method: a case study for AISI H13 tool steel. *Int J Adv Manuf Technol* 58(1):201–209
114. Mia M, Razi MH, Ahmad I, Mostafa R, Rahman SMS, Ahmed DH, Dey PR, Dhar NR (2017) Effect of time-controlled MQL pulsing on surface roughness in hard turning by statistical analysis and artificial neural network. *Int J Adv Manuf Technol* 91(9):3211–3223
115. Hassan MH, Othman AR, Kamaruddin S (2017) The use of response surface methodology (RSM) to optimize the acid digestion parameters in fiber volume fraction test of aircraft composite structures. *Int J Adv Manuf Technol* 90(9):3739–3748
116. Mia M, Bashir MA, Khan MA, Dhar NR (2017) Optimization of MQL flow rate for minimum cutting force and surface roughness in end milling of hardened steel (HRC 40). *Int J Adv Manuf Technol* 89(1):675–690
117. Azam M, Jahanzaib M, Wasim A, Hussain S (2015) Surface roughness modeling using RSM for HSLA steel by coated carbide tools. *Int J Adv Manuf Technol* 78(5):1031–1041
118. Box GE, Behnken DW (1960) Some new three level designs for the study of quantitative variables. *Techno Metrics* 2(4):455–475
119. Montgomery DC (2001) *Design and analysis of experiments*, 5th edn. Wiley, New York
120. Senthilkumar N, Tamizharasan T, Anandkrishnan V (2013) An ANN approach for predicting the cutting inserts performances of different geometries in hard turning. *Adv Prod Eng Manag* 8(4)
121. Kapgate RA, Tatwawadi VH (2013) Artificial neural network modelling for wire-EDM processing of aluminium silicon carbide metal matrix composite. *Int J Eng Res Technol* 2(5):2249–2256
122. Joshi SN, Pande SS (2011) Intelligent process modeling and optimization of die-sinking electric discharge machining. *Appl Soft Comput* 11(2):2743–2755
123. Mohanty A, Talla G, Gangopadhyay S (2014) Experimental investigation and analysis of EDM characteristics of Inconel 825. *Mater Manuf Process* 29(5):540–549
124. Shirguppikar SS, Patil MS, Ganachari VS, Kolekar TV, Jadhav PS, Chougule AB (2018) Experimental investigation of CNT coated tools for EDM processes. *Mater Today: Proc* 5(2):7131–7140
125. Unune DR, Mali HS (2018) Experimental investigation on low-frequency vibration-assisted  $\mu$ -ED milling of Inconel 718. *Mater Manuf Process* 33(9):964–976

**Publisher's Note** Springer Nature remains neutral with regard to jurisdictional claims in published maps and institutional affiliations.